Towards Integrated Type and Dimensional Synthesis of Mechanisms for Rigid Body Guidance

M.J.D. Hayes[1], P.J. Zsombor-Murray[2]

[1]*Department of Mechanical & Aerospace Engineering, Carleton University, 1125 Colonel By Drive, Ottawa, ON, K1S 5B6, Canada,*
jhayes@mae.carleton.ca

[2]*Centre for Intelligent Machines, McGill University, 817 Sherbrooke Street West, Montreal, QC, H3A 2K6, Canada*
paul@cim.mcgill.ca

In this paper kinematic mapping is used to take the first steps towards development of a general algorithm combining both type and dimensional synthesis of planar mechanisms for rigid body guidance. In the present work we develop an algorithm that can size link lengths, locate joint axes, and using heuristics decide between RR- and PR-dyads that, when combined, can guide a rigid body exactly through five specified positions and orientations, i.e., the five-position Burmester problem. An example is given providing proof-of-concept.

1 Introduction

The determination of a planar four-bar mechanism that can guide a rigid body through five finitely separated *poses* (position and orientation) is known as the *five-position Burmester problem*. It may be stated as follows: given five positions of a point on a moving rigid body and the corresponding five orientations of some line on that body, design a four-bar mechanism whose coupler is the moving body and is assemblable upon these five poses. The coupler must assume the five required poses, even though it may be that not all five lie in the same assembly branch. Burmester showed that the problem leads to, at most, four dyads that can be taken two at a time: there can be as many as six different four-bar mechanisms that can guide a rigid body exactly through five specified poses [1].

From time to time dimensional synthesis for the Burmester problem has been revisited, see for example [2]. More recently, classical finite position synthesis has been reviewed in [3]. An algebraic approach to this exact problem based on quaternions is to be found in [4]. Instead, we use planar kinematic mapping whose geometry is analogous to quaternions. The planar kinematic mapping was introduced independently by Blaschke and Grünwald in 1911 [5, 6], and is summarized in [7].

In general, dimensional synthesis for rigid body guidance assumes a mechanism *type*: i.e., planar $4R$; slider-crank; crank-slider; trammel, etc.. Our aim is to develop a completely general planar mechanism synthesis algorithm that integrates both *type* and *dimensional* synthesis for five-position exact synthesis. It was shown in [8] how kinematic mapping can be used for exact dimensional synthesis.

We employ the Blashke-Grünwald mapping of planar kinematics [5, 6] to regard the problem from a projective geometric perspective, thereby obtaining a system of five non-linear equations in five unknowns expressed in terms of a sixth *homogenizing*, or *influence coefficient*. The value of the sixth unknown determines *type*. The six unknowns represent one dyad. The solutions of the system of equations leads to, at most, four dyads, thereby agreeing with Burmester theory.

It is convenient to characterize rigid body displacements by a coordinate system E that moves relative to a fixed coordinate system Σ, see Figure 1. General planar displacements are then the transformation of points described in E to the coordinates of the same points described in Σ. The constraints on linkages imposed by different joint types can then be described geometrically.

Planar linkages contain either revolute (R-pairs), or prismatic (P-pairs). These kinematic pairs permit rotations about one axis, or translations parallel to one direction, respectively. In the kinematic mapping image space an RR-dyad (three binary links jointed end to end by two R-pairs) constraint involving a point with fixed coordinates in E forced to move on a circle with fixed radius and centre in

Σ is a hyperboloid of one sheet. A PR-dyad (three binary links jointed in series by a P-pair and an R-pair) imposes the constraint where a point with fixed coordinates in E is restricted to move on a line with fixed line coordinates in Σ. This constraint maps to a hyperbolic paraboloid in the image space. The RP-dyad is the kinematic inversion of the PR-dyad. It's constraints also map to hyperbolic paraboloids. The PP-dyad constraints map to a plane in the image space. These are the four possible lower pair dyads for planar mechanisms.

The algorithm that performs both type and dimensional synthesis for rigid body guidance must identify the constraint surfaces that intersect in the curve specified by the image space points of the five given poses. The way the constraints are formulated, the influence coefficient, mentioned earlier, can have either the value 1 or 0, indicating either an RR- or PR-dyad, respectively.

The planar $RRRP$ four-bar linkage shown in Figure 1 can be decomposed into an RR- and a PR-dyad. The RR-dyad is composed of the grounded R-pair centred at the base-fixed point F_1 and the moving R-pair centred at the point M_1. The PR-dyad is composed of the sliding P-pair and the R-pair connected to it with centre at M_2. In the PR-dyad, the P-pair slides on a line with fixed position and direction relative to the base-fixed R-pair centred at F_1. This $RRRP$ linkage is used to generate the five specified poses. Clearly, the algorithm must identify the constraint surfaces corresponding to the given RR- and PR-dyads. Using heuristics, we succeed in identifying these dyads, together with two additional RR-dyads, thereby agreeing with Burmester theory. These are the first steps towards the general algorithm.

2 Kinematic Mapping

The motion of the coupler in a four-bar mechanism can be described by the motion of a reference frame E that moves with the coupler, relative to a ground-fixed non moving reference frame Σ. The $RRRP$ linkage shown in Figure 1 illustrates these two coordinate reference frames. The homogeneous coordinates of points represented in E are given by the ratios $(x : y : z)$. Those of points represented in Σ are given by the ratios $(X : Y : Z)$.

The homogeneous transformation that maps the coordinates of points in E to Σ, which also describes the displacement of E relative to Σ, can be written:

$$\begin{bmatrix} X \\ Y \\ Z \end{bmatrix} = \begin{bmatrix} \cos\varphi & -\sin\varphi & a \\ \sin\varphi & \cos\varphi & b \\ 0 & 0 & 1 \end{bmatrix} \begin{bmatrix} x \\ y \\ z \end{bmatrix}. \qquad (1)$$

Equation (1) indicates that general planar displacements are characterized by the three parameters a, b, and φ, where the pair (a, b) are the $(X/Z, Y/Z)$ Cartesian coordinates of the origin of E expressed in Σ, and φ is the orientation of E relative to Σ, respectively.

All general planar displacements (*i.e.*, any combination of translations and rotations) may be represented by a single rotation through a finite angle about a fixed axis normal to the plane of the displacement. Even a pure translation may be considered a rotation through an infinitesimal angle about the point at infinity in the direction normal to the translation. The coordinates of the piercing point of the rotation axis with the plane of the displacement describe the *pole* of the displacement. The coordinates of the pole are invariant under the associated transformation described by Equation (1).

The pole coordinates for a particular displacement come from the eigenvector corresponding to the one real eigenvalue of Equation (1). Denoting them by the subscript p, the homogeneous pole coordinates, which are the same in both E and Σ, are:

$$\begin{aligned} X_p = \quad x_p = \quad & a\sin(\varphi/2) - b\cos(\varphi/2), \\ Y_p = \quad y_p = \quad & a\cos(\phi/2) + b\sin(\varphi/2), \\ Z_p = \quad z_p = \quad & 2\sin\varphi/2. \end{aligned}$$

Note that the value of the homogenizing coordinate is arbitrary. Without loss in generality it is set $Z_p = z_p = 2\sin\varphi/2$.

The essential idea of kinematic mapping is to map the three homogeneous coordinates of the pole of a planar displacement, in terms of three parameters that characterize it, (a, b, φ), to the points of a three dimensional projective image space. The kinematic mapping image coordinates are defined as:

$$\begin{aligned} X_1 &= a\sin(\varphi/2) - b\cos(\varphi/2) \\ X_2 &= a\cos(\varphi/2) + b\sin(\varphi/2) \\ X_3 &= 2\sin(\varphi/2) \\ X_4 &= 2\cos(\varphi/2). \end{aligned} \qquad (2)$$

Since each distinct displacement described by (a, b, φ) has a corresponding unique image point, the inverse mapping can be obtained from Equation (2): for a given point of the image space, the displacement parameters are

$$\begin{aligned} \tan(\varphi/2) = X_3/X_4, \\ a = 2(X_1X_3 + X_2X_4)/(X_3^2 + X_4^2), \\ b = 2(X_2X_3 - X_1X_4)/(X_3^2 + X_4^2). \end{aligned} \qquad (3)$$

By virtue of the relationships expressed by Equations (2), the transformation matrix from Equation (1) may be expressed in terms of the homogeneous coordinates of the image space. This yields a

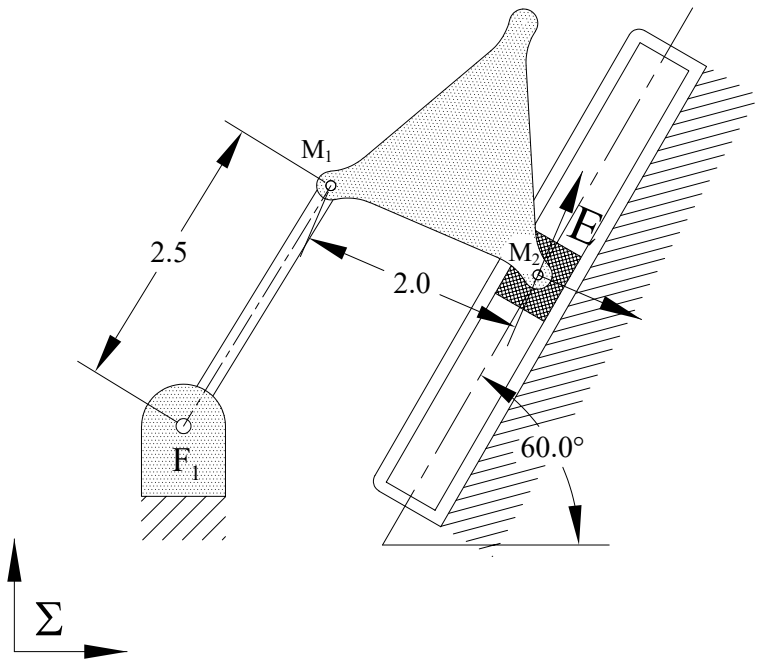

Figure 1: $RRRP$ linkage used to generate the five poses for the example.

linear transformation to express a displacement of E with respect to Σ in terms of the image point [7]:

$$\lambda \begin{bmatrix} X \\ Y \\ Z \end{bmatrix} = \boldsymbol{T} \begin{bmatrix} x \\ y \\ z \end{bmatrix}, \tag{4}$$

where λ is some non-zero constant arising from the use of homogeneous coordinates and

$$\boldsymbol{T} = \begin{bmatrix} X_4^2 - X_3^2 & -2X_3X_4 & 2(X_1X_3 + X_2X_4) \\ 2X_3X_4 & X_4^2 - X_3^2 & 2(X_2X_3 - X_1X_4) \\ 0 & 0 & X_3^2 + X_4^2 \end{bmatrix}.$$

The inverse transformation can be obtained with the inverse of the matrix in Equation (4) as follows.

$$\gamma \begin{bmatrix} x \\ y \\ z \end{bmatrix} = \boldsymbol{T}^{-1} \begin{bmatrix} X \\ Y \\ Z \end{bmatrix}, \tag{5}$$

with γ being another non-zero constant arising from the use of homogeneous coordinates and

$$\boldsymbol{T}^{-1} = \begin{bmatrix} X_4^2 - X_3^2 & 2X_3X_4 & 2(X_1X_3 - X_2X_4) \\ -2X_3X_4 & X_4^2 - X_3^2 & 2(X_2X_3 + X_1X_4) \\ 0 & 0 & X_3^2 + X_4^2 \end{bmatrix}.$$

2.1 Kinematic Constraints

There is a specific type of constrained motion corresponding to each type of planar lower-pair dyad: RR-type; PR-type; RP-type; and PP-type. Because a motion is a continuous set of displacements, and because a displacement maps to a point, a constrained motion will map to a continuous set of points in the image space. As shown in [9], the constraints imposed by the four different dyad types are quadric surfaces with special properties in the image space.

A clearer picture of the image space constraint surface that corresponds to the possible kinematic constraints emerges when $(X : Y : Z)$, or $(x : y : z)$ from Equations (4), or (5) are substituted into the general equation of a circle, the form of the most general constraint [10]:

$$K_0(X^2+Y^2)+2K_1XZ+2K_2YZ+K_3Z^2 = 0. \tag{6}$$

The K_i in Equation (6) depend on the constraint imposed by the dyad. The result is that the constraint surfaces corresponding to RR, PR, and RP-dyads can be represented by *one* equation [10]. It is obtained by substituting the results from Equations (4), or (5) into Equation (6). However, the expression is greatly simplified under the following assumptions:

1. No mechanism of practical significance will have a point at infinity, so it is safe to set $z = 1$.

2. Coupler rotations of $\varphi = \pi$ (half-turns) have images in the plane $X_4 = 0$. Because the X_i are implicitly defined by Equation (2), setting $\varphi = \pi$ gives

$$(X_1 : X_2 : X_3 : X_4) = (a : b : 2 : 0). \tag{7}$$

When we remove the one parameter family of image points for coupler orientations of $\varphi = \pi$ we can, for convenience, normalise the image space coordinates by setting $X_4 = 1$. Conceptually, this implies dividing the X_i by $X_4 = 2\cos\varphi/2$ giving

$$\begin{aligned} X_1 &= \frac{1}{2}\left(a\tan(\varphi/2) - b\right) \\ X_2 &= \frac{1}{2}\left(a + b\tan(\varphi/2)\right) \\ X_3 &= \tan(\varphi/2) \\ X_4 &= 1. \end{aligned} \tag{8}$$

Applying these assumptions to Equations (4), or (5) gives the simplified constraint surface equation upon substitution in Equation (6):

$$\begin{aligned} &K_0(X_1^2 + X_2^2) + (-K_0x + K_1)X_1X_3 \\ &+(-K_0y + K_2)X_2X_3 \mp (K_0y + K_2)X_1 \\ &\pm(K_0x + K_1)X_2 \mp (K_1y - K_2x)X_3 \\ &+\tfrac{1}{4}[K_0(x^2 + y^2) - 2(K_1x + K_2y) + K_3]X_3^2 \\ &+\tfrac{1}{4}[K_0(x^2 + y^2) + 2(K_1x + K_2y) + K_3] = 0. \end{aligned} \tag{9}$$

The X_i are the image space coordinates that represent a displacement of E relative to Σ. The x and y, after setting $z = 1$, are the Cartesian coordinates of the coupler attachment point in E. For both the RR- and PR-dyads the coupler and base-fixed link are joined by an R-pair, hence these coordinates are conveniently selected to be the rotation centre of the R-pair. The constraint surfaces for these dyads are obtained by using the *upper* signs in Equation (9). Note that for RP-dyads the kinematic constraint is inverted: instead of an R-pair centre constrained to move along a fixed line yielding a fixed range of points, we have a movable line constrained to move on a fixed point yielding a planar pencil of lines on the fixed point. For this case we use the alternate form of Equation (9) where the coordinates $(X : Y : 1)$ of the fixed R-pair centre are used in place of $(x : y : 1)$, and the *lower* signs are used. See [10] for a detailed explanation.

PP-dyads represent a special case. The image space constraint surface corresponding to possible displacements of a PP-dyad is a degenerate quadric that splits into a real and an imaginary plane. This is because only curvilinear motion of the coupler can result. Because φ is constant, the image space coordinates $X_3 = f(\varphi)$ and $X_4 = g(\varphi)$ must also be constant. Hence, the finite part of the two dimensional constraint manifold is linear and must be a hyper-plane. The plane is completely determined by the coupler orientation. When the image space is normalised by setting $X_4 = 1$, the surface equation is simply $X_3 = \tan(\varphi/2)$.

In what follows only RR- and PR-dyads will be considered to provide some degree of *proof-of-concept*. Development, refinement, and generalization of this approach will come in subsequent publications.

2.2 RR-type Circular Constraints

The ungrounded R-pair in an RR-dyad is constrained to move on a circle with a fixed centre. Meanwhile, the coupler can rotate about the moving R-pair when the coupler connection to the other dyad has been removed. This two parameter family of displacements corresponds to a two parameter hyperboloid of one sheet in the image space. An important property of the hyperboloid is that sections in planes parallel to $X_3 = 0$ are circles [9]. Each one of these image space circles represents possible coupler displacements with a fixed orientation. Thus the constraints imposed by RR-dyads are called *circular constraints*. The exact coefficients of the hyperboloid are determined by substituting in Equation (9) the appropriate values for the kinematic parameters:

$$\begin{aligned} K_0 &= 1, \\ K_1 &= -X_c, \\ K_2 &= -Y_c, \\ K_3 &= K_1^2 + K_2^2 - r^2, \end{aligned} \tag{10}$$

where (X_c, Y_c) are the Cartesian coordinates of the fixed circle centre in the reference frame that is considered to be non-moving, and r is the circle radius. If the kinematic constraint is a fixed point in E bound to fixed circle in Σ, then (x, y) are the Cartesian coordinates of the coupler reference point in E, and the upper signs apply. If the kinematic constraint is a fixed point in Σ bound to fixed circle in E, then (X, Y) are substituted for (x, y) as the coordinates of the coupler reference point in Σ, and the lower signs apply.

2.3 PR-type Linear Constraints

Linear constraints result when PR- and RP-dyads are employed. The linear coefficients are defined as

$$[K_0 : K_1 : K_2 : K_3] = [0 : \tfrac{1}{2}L_1 : \tfrac{1}{2}L_2 : L_3], \tag{11}$$

where the L_i are line coordinates obtained by Grassmann expansion of the determinant of any two distinct points on the line [11].

Of these in the present work we consider only PR-dyads. The direction of the line is a design constant, described by the angle it makes with respect to the fixed base frame Σ, indicated by ϑ_Σ. The point at infinity contained on the line is determined by the

direction of the line, and hence can be specified as $(\cos\vartheta_\Sigma : \sin\vartheta_\Sigma : 0)$. Additionally, the location of a fixed point on the line, also expressed in Σ, is given by the coordinates F_Σ. The line equation in Σ for a given PR-dyad is obtained from the Grassmann expansion:

$$\begin{vmatrix} X & Y & Z \\ F_{X/\Sigma} & F_{Y/\Sigma} & F_{Z/\Sigma} \\ \cos\vartheta_\Sigma & \sin\vartheta_\Sigma & 0 \end{vmatrix} = 0, \qquad (12)$$

where the notation $F_{X/\Sigma}$, $F_{Y/\Sigma}$, $F_{Z/\Sigma}$, represent the homogeneous coordinates $(X : Y : Z)$, expressed in reference frame Σ, of a fixed point on the line that is fixed relative to Σ. Applying Equations (11) and (12) we obtain

$$\begin{aligned} K_0 &= 0, \\ K_1 &= -\frac{F_{Z/\Sigma}}{2}\sin\vartheta_\Sigma, \\ K_2 &= \frac{F_{Z/\Sigma}}{2}\cos\vartheta_\Sigma, \\ K_3 &= F_{X/\Sigma}\sin\vartheta_\Sigma - F_{Y/\Sigma}\cos\vartheta_\Sigma. \end{aligned} \qquad (13)$$

The direction of the translation permitted by the P-pair is specified by the angle the line makes expressed in Σ, ϑ_Σ. When the coordinates of a fixed point on the line are known, we obtain the line coefficients $[K_0 : K_1 : K_2 : K_3]$. These, along with the design values of the coordinates of the coupler attachment point (x, y), expressed in reference frame E, substituted into Equation (9) reveals the image space constraint surface for the given PR-dyad. This surface is an hyperbolic paraboloid [9] with one regulus ruled by skew lines that are all parallel to the plane $X_3 = 0$.

2.4 The Burmester Problem in the Image Space

Each specified pose of E determines a point, $(X_1 : X_2 : X_3 : X_4)$, in the image space. If the displacements are feasible, the five points lie on the curve of intersection of the dyad constraint surfaces. The five points are enough to determine the intersecting quadrics. Recall that, in general, nine points are required to specify a quadric. The special nature of the constraint surfaces represent four constraints on these quadrics.

The hyperboloids, corresponding to RR-dyads, intersect planes parallel to $X_3 = 0$ in circles. Thus, all constraint hyperboloids contain the image space equivalent of the *imaginary circular points*, J_1 and J_2: $(1 : \pm i : 0 : 0)$. The points J_1 and J_2 are imaginary points on the real line, l, of intersection of the planes $X_3 = 0$ and $X_4 = 0$. This real line is the axis of a pencil of planes that includes the complex conjugate planes V_1 and V_2, defined by: $X_3 = \pm iX_4$. The hyperboloids all have V_1 and V_2 as tangent planes, though not necessarily at J_1 and J_2.

The hyperbolic paraboloids, corresponding to PR- and RP-dyads, contain l as a generator. Therefore all constraint hyperbolic paraboloids contain J_1 and J_2, moreover V_1 and V_2 are the tangent planes at these two points. Thus every constraint surface for RR-, PR-, and RP-dyads have these four conditions in common, reducing the number of independent parameters to five.

Our approach is to leave K_0 as an unspecified variable homogenizing coordinate and solve the synthesis equations in terms of K_0. In general, the constants K_1, K_2, and K_3 will depend on K_0. If these multipliers become very large (on the order of 10^6) indicating a very large crank radius then we set $K_0 = 0$ and use line coordinate definitions for K_1, K_2, and K_3 in Equation 13 giving a PR-dyad. Otherwise, $K_0 = 1$, and the circle coordinate definitions for K_1, K_2, and K_3 in Equation 10 are used yielding an RR-dyad.

3 Example

The mechanism illustrated in Figure 1 was used to generate the five poses listed in Table 1 and displayed in Figure 2. For this generating mechanism, the origin of reference frame E, O_E, is on the centre of the R-pair on the coupler point M_2. Homogeneous coordinates in E are described by the triples of ratios $(x : y : z)$. The coupler reference points M_1 and M_2 define the direction of the x-axis. The positive y-axis is as shown in Figures 1 and 2. Frame Σ is as shown in the same two figures. Reference frame E moves with the coupler. The fixed R-pair center is located on point F_1. The geometry of the generating mechanism is listed in the right hand side of Table 1.

The given five poses are mapped to the coordinates of five points in the image space. Using a computer algebra software package, we substitute the corresponding values for X_1, X_2, X_3, together with $X_4 = 1$ and $z = 1$ into Equation (9), effectively projecting the points onto the embedded Euclidean Space. This produces the following five nonlinear equations in terms of K_0, K_1, K_2, K_3, x, and y, which are quadratic when K_0 is considered constant:

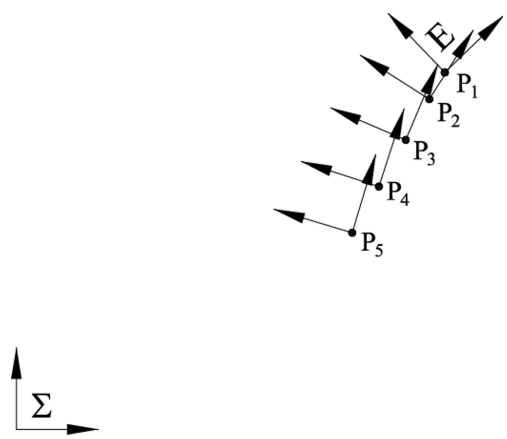

Figure 2: The five poses.

pose	a	b	φ (deg)	parameter	value
1	5.24080746	4.36781272	43.88348278	F_1	$(X:Y:Z)=(1.5:2:1)$
2	5.05087057	4.03883237	57.45578356	M_1	$(x:y:z)=(-2:0:1)$
3	4.76358093	3.54123213	66.99534998	M_2	$(x:y:z)=(0:0:1)$
4	4.43453496	2.97130779	72.10014317	M_1M_2	$l=2$
5	4.10748142	2.40483444	72.30529428	F_1M_1	$r=2.5$
				P-pair angle	$\vartheta_\Sigma=60$ (deg)

Table 1: Five poses of the $RRRP$ mechanism; Geometry of the $RRRP$ generating mechanism.

$$\begin{gathered}(13.52428430+3.954702976x-0.281732470y+0.2905708072x^2+0.2905708072y^2)K_0+\\(3.045651308+0.4188583855x-0.4028439264y)K_1+\\(2.538317736+0.4028439264x+0.4188583855y)K_2+0.2905708072K_3;\end{gathered}\tag{14}$$

$$\begin{gathered}(13.59714292+3.980465638x-1.355748810y+0.3251080324x^2+0.3251080324y^2)K_0+\\(3.284157186+0.3497839351x-0.5481168944y)K_1+\\(2.626113690+0.3497839351y+0.5481168944x)K_2+0.3251080324K_3;\end{gathered}\tag{15}$$

$$\begin{gathered}(12.66604850+3.682213684x-2.157608235y+0.3595038128x^2+0.3595038128y^2)K_0+\\(3.425051014+0.2809923744x-0.6618272064y)K_1+\\(2.546172905+0.6618272064x+0.2809923744y)K_2+0.3595038128K_3;\end{gathered}\tag{16}$$

$$\begin{gathered}(10.89749412+3.205294435x-2.529259406y+0.3824518134x^2+0.3824518134y^2)K_0+\\(3.391991875+0.2350963732x-0.7278785984y)K_1+\\(2.272764106+0.7278785984x+0.2350963732y)K_2+0.3824518134K_3;\end{gathered}\tag{17}$$

$$\begin{gathered}(8.686958330+2.714462017x-2.440453512y+0.3834517468x^2+0.3834517468y^2)K_0+\\(3.150041851+0.2330965065x-0.7306209600y)K_1+\\(+1.844275934+0.7306209600x+0.2330965065y)K_2+0.3834517468K_3;\end{gathered}\tag{18}$$

Parameter	Surface 1	Surface 2	Surface 3	Surface 4
K_1	$-1.500K_0$	$-4.2909 \times 10^6 K_0$	$-15.6041K_0$	$-8.3011K_0$
K_2	$-2.0000K_0$	$2.4773 \times 10^6 K_0$	$3.4362K_0$	$-5.0837K_0$
K_3	$-2.5801 \times 10^{-6} K_0$	$2.3334 \times 10^7 K_0$	$107.3652K_0$	$93.4290K_0$
x	-2.0000	8.1749×10^{-7}	0.2281	3.7705
y	3.4329×10^{-7}	-1.3214×10^{-6}	-0.7845	-2.0319

Table 2: The identified constraint surface coefficients.

Parameter	Relation	Value
F_1	$(-K_{1_1}, -K_{2_1})$	$(1.500, 2.000)$
M_1	(x_1, y_1)	$(-2.000, 3.4329 \times 10^{-7})$
M_2	(x_2, y_2)	$(8.1749 \times 10^{-7}, -1.3214 \times 10^{-6})$
ϑ_Σ	$\arctan\left(\frac{-K_{1_2}}{K_{2_2}}\right)$	$60.0°$

Table 3: Geometry of one of six synthesized mechanisms that is a good approximation of the generating $RRRP$ linkage in Figure 1.

Solving the system of Equarions (14-18) for the unknowns K_1, K_2, K_3, x, and y in terms of K_0 yields the set of four solutions listed in Table 2. Substituting these values into Equation (9) gives four distinct constraint surfaces in the image space, in terms of the homogenizing circle, or line coordinate, K_0.

At the present time, heuristics must be used to select an appropriate value for K_0 by comparing the relative magnitudes of K_1 and K_2. Recall that the circle coordinates are defined to be $K_1 = -X_c$, and $K_2 = -Y_c$, the Cartesian coordinates of the fixed revolute centres, multiplied by -1, expressed in Σ. The crank radius is given by $r = +\sqrt{K_3^2 - (K_1^2 + K_2^2)}$. The coefficients for Surfaces 1, 3, and 4 represent RR-dyads with finite rotation centres when $K_0 = 1$. However, the coefficients for Surface 2, relative to the other three, have a rotation centre whose location approaches infinity, $(4.2909 \times 10^6, -2.4773 \times 10^6)$ with a crank radius of 4.9547×10^6, also approaching infinity, while the relative values of x and y indicate this attachment point is on O_E. This surface should clearly be recomputed as an hyperbolic paraboloid revealing the corresponding PR-dyad. Recall the line coordinate definition, with K_0 left unspecified:

$$\begin{aligned} K_0 &= K_0, \\ K_1 &= -\frac{F_{Z/\Sigma}}{2} \sin \vartheta_\Sigma, \\ K_2 &= \frac{F_{Z/\Sigma}}{2} \cos \vartheta_\Sigma, \\ K_3 &= F_{X/\Sigma} \sin \vartheta_\Sigma - F_{Y/\Sigma} \cos \vartheta_\Sigma. \end{aligned} \quad (19)$$

The angle of the direction of translation of the P-

Solution	Dyad surface pairing
1	Dyad 1 - Dyad 2
2	Dyad 2 - Dyad 3
3	Dyad 2 - Dyad 4
4	Dyad 1 - Dyad 3
5	Dyad 1 - Dyad 4
6	Dyad 3 - Dyad 4

Table 4: Dyad pairings yielding the six synthesized mechanisms.

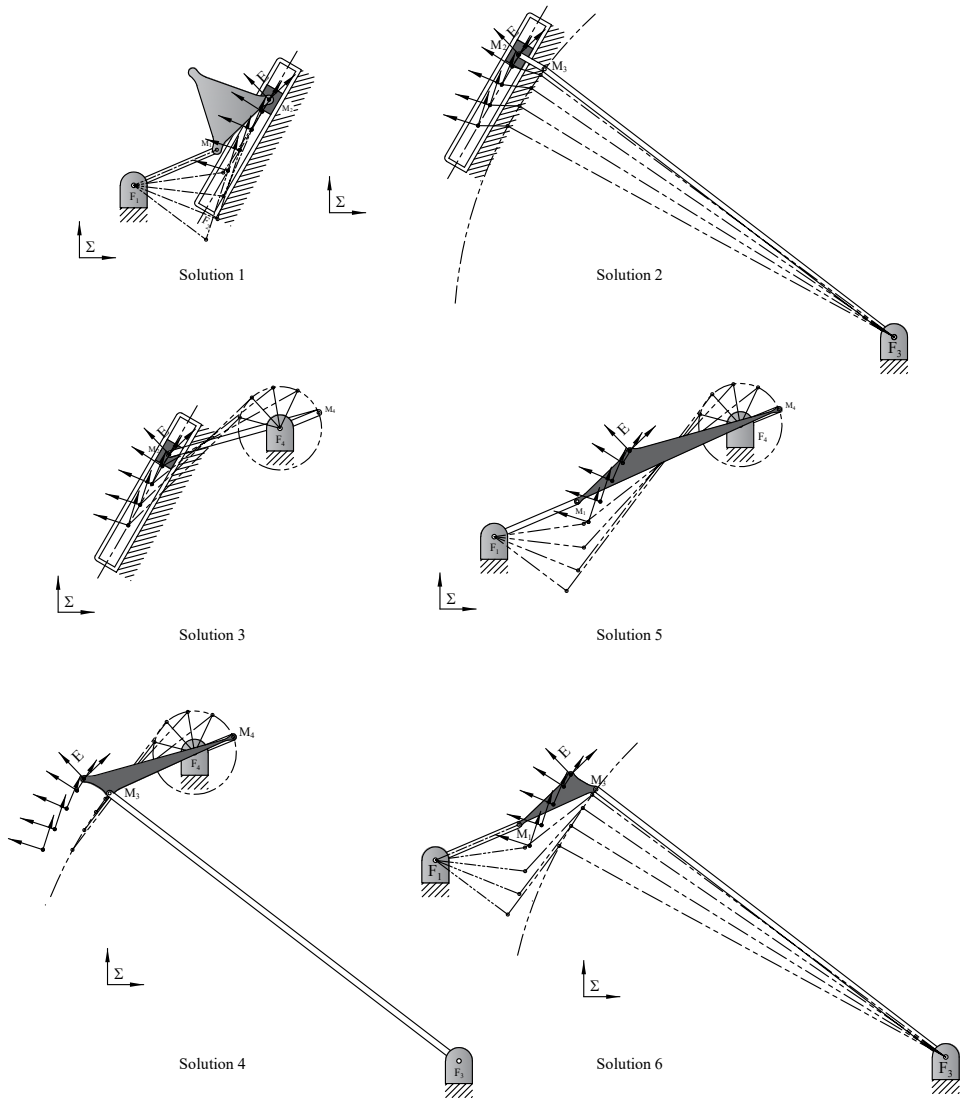

Figure 3: The six synthesized mechanisms.

pair relative to the X-axis of Σ is ϑ_Σ. The translation direction of a PR-dyad that could be combined with any of the three RR-dyads is thus

$$\begin{aligned}\vartheta_\Sigma &= \arctan\left(\frac{-K_1}{K_2}\right)\\ &= \arctan\left(\frac{4.2909\times 10^6 K_0}{2.4773\times 10^6 K_0}\right)\\ &= 60.0^\circ. \qquad (20)\end{aligned}$$

Employing plane trigonometry, it is simple to extract the link lengths and joint locations of the dyad associated with each of the four constraint surfaces. The generating mechanism is reproduced when the dyads corresponding to Surfaces 1 and 2 are paired. We obtain the geometry listed in Table 3 (note, the second subscript refers to the particular surface). The six possible mechanisms are the combinations of the four dyads taken two at a time. These are listed in Table 4 and are illustrated in Figure 3.

4 Conclusions

The example presented herein illustrates that the general image space constraint surface equation, leaving K_0 unspecified, can be used for general type and dimensional synthesis for planar mechanisms. For a set of five poses generated by a particular slider-crank, we synthesized six mechanisms, including the one that generated the poses, that can

guide the coupler through the five poses. Three of the six synthesized linkages are slider-cranks while the remaining three are $4R$ mechanisms. The coupler point is the centre of the R-pair connecting the coupler to the P-pair. This coupler point is clearly bound to a line in the $RRRP$ linkages, but not in the case of the $4R$'s. This approach to planar four-bar mechanisms stands to offer the designer *all* possible linkages that can attain the desired poses, not just $4R$'s and not just slider-cranks, but *all* feasible four-bar linkage architectures along with their dimensions.

Outstanding issues involve the following. The heuristics must be rethought so that an algorithm for type selection can be developed. Moreover, the problem formulation must be reconsidered in such a way that both PR- and RP-dyads can be typed, and extracted from the solutions. The geometric reasoning explaining why five image space points are sufficient to define four unique quadrics must be formalized. Additionally, the geometric interpretation of K_0 must be investigated. How, for example, are the constraint hyperbolic paraboloids parameterized in the image space without setting $K_0 = 0$?

Finally, methods to apply this technique to approximate synthesis should be investigated. The resulting problem would involve fitting a suitable number of points to surfaces in the image space. More specifically, fitting points to the curve of intersection of constraint surfaces. To do this some form of least-squares error minimization would have to be employed. The outcome would be a single dyad pair: the one corresponding to the two constraint surfaces whose intersection best approximates the given set of desired poses

References

[1] L. Burmester. *Lehrbuch der Kinematik*. Arthur Felix Verlag, Leipzig, Germany, 1888.

[2] Y.C. Ching, J. Angeles, and M. González-Palacios. "A Semi-graphical Method for the Solution of the BurmesterProblem". *ASME Adv. in Des. Auto.*, DE-Vol. 32-2: pages 321–326, 1991.

[3] J.M. McCarthy. *Geometric Design of Linkages*. Springer-Verlag, New York, N.Y., U.S.A., 2000.

[4] A.P. Murray and J.M. McCarthy. "Constraint Manifold Synthesis of Planar Linkages". *Proceedings of ASME DETC: Mechanisms Conference, Irvine CA.*, 1996.

[5] W. Blaschke. "Euklidische Kinematik und Nichteuklidische Geometrie". *Zeitschr. Math. Phys.*, vol. 60: pages 61–91 and 203–204, 1911.

[6] J. Grünwald. "Ein Abbildungsprinzip, welches die ebene Geometrie und Kinematik mit der räumlichen Geometrie verknüpft". *Sitzber. Ak. Wiss. Wien*, vol. 120: pages 677–741, 1911.

[7] O. Bottema and B. Roth. *Theoretical Kinematics*. Dover Publications, Inc., New York, N.Y., U.S.A., 1990.

[8] M.J.D. Hayes and P.J. Zsombor-Murray. "Solving the Burmester Problem Using Kinematic Mapping". *Proc. of the ASME Design Engineering Technical Conferences: Mechanisms Conference,* Montréal, QC, Canada, on CD, Sept. 2002.

[9] M.J.D. Hayes and M.L. Husty. "On the Kinematic Constraint Surfaces of General Three-Legged Planar Robot Platforms". *Mechanism and Machine Theory*, vol. 38, no. 5: pages 379–394, 2003.

[10] M.J.D. Hayes, P.J. Zsombor-Murray, and C. Chen. "Kinematic Analyais of General Planar Parallel Manipulators". *ASME, Journal of Mechanical Design*, in-press, 2004.

[11] F. Klein. *Elementary Mathematics from an Advanced Standpoint: Geometry*. Dover Publications, Inc., New York, N.Y., U.S.A., 1939.